Kinetic properties of the mitochondrial F1FO-ATPase activity elicited by Ca2+ in replacement of Mg2+

Kinetic properties of the mitochondrial F_1F_O-ATPase activity elicited by Ca^{2+} in replacement of Mg^{2+}

Salvatore Nesci, Fabiana Trombetti, Vittoria Ventrella, Maurizio Pirini, Alessandra Pagliarani*

Department of Veterinary Medical Sciences (DIMEVET), University of Bologna, via Tolara di Sopra 50, 40064 Ozzano dell'Emilia (BO) – Italy.

*Corresponding author: Alessandra Pagliarani alessandra.pagliarani@unibo.it
Tel. +39 051 2097017
Fax. +39 051 2086178

Salvatore Nesci designed the experiments. All other authors equally contributed to this work.

Abstract

The mitochondrial F-ATPase can be activated either by the classical cofactor Mg^{2+} or, with lower efficiency, by Ca^{2+}. The latter may play a role when calcium concentration rises in mitochondria, a condition associated with cascade events leading to cell death. Common and distinctive features of these differently activated mitochondrial ATPases were pointed out in swine heart mitochondria. When Ca^{2+} replaces the natural cofactor Mg^{2+}, the enzyme responsiveness to the transmembrane electrochemical gradient and to the classical F-ATPase inhibitors DCCD and oligomycin as well as the oligomycin sensitivity loss by thiol oxidation, are maintained. Consistently, the two mitochondrial ATPases apparently share the F_1F_O complex basic structure and mechanism. Peculiar cation-dependent properties, which may affect the F_1 catalytic mechanism and/or the F_O proton binding site features, may be linked to a different physiological role of the mitochondrial Ca-activated F-ATPase with respect to the Mg-activated F-ATPase

Keywords

Mitochondrial F_1F_O-ATPase; calcium cofactor; kinetic properties.

Abbreviations

IO-SMP, inside-out submitochondrial particles; PTP, permeability transition pore; DNP, α-Dinitrophenol; DTE, 1,4-Dithioerythritol; DCCD, *N*,*N*′-dicyclohexylcarbodiimide; k_{DCCD}, rate constant of DCCD inhibition; TBT, tributyltin; Succ, succinate; ROT, rotenone.

1. Introduction

The ubiquitous F_1F_O-ATPase has the main task of synthesing ATP in the cell of all the living organisms [1] by coupling the two opposite functions of ATP synthesis and hydrolysis to the different electrochemical membrane proton gradient. This reversible and biologically unique energy-transducing mechanism made the enzyme complex fully deserve the definition of "a splendid molecular machine" [2]. Structurally, the F_1F_O-ATPase is a multi-subunit complex which basically consists of a water-soluble F_1 catalytic domain and a membrane-inserted F_O domain, mutually connected by a central and a peripheral stalk [3]. F_1 is a sort of globular hexamer in which three *α*-subunits with three non-catalytic sites alternate with three *β*-subunits bearing three catalytic sites [4]. In F_O the *c*-ring constitutes the rotor. The central stalk links F_O rotation to catalysis, while laterally the peripheral stalk stabilizes the torque generation of the rotor [5]. The rotation is driven by the proton flux through the *c*-ring and the *a* subunit interface. The latter is a quite mysterious entity [6] which not only determines the rotation direction of the rotor [7], but also drives H^+ binding to the *c*-ring proton-binding site an Glu carboxylate. The interplay between the protonated and de-protonated Glu form in turn allows the transmembrane proton translocation [8]. Any 360° rotation which produces 3 ATP molecules implies that the three catalytic sites of F_1 undergo three functional states with increasing affinity for ATP, named β_E, β_{DP} and β_{TP}, respectively [9]. It is long known that the nucleotide binding to the *β*-subunit requires the coordination of the essential cofactor Mg^{2+}, which contributes to the catalytic site asymmetry producing the different affinities for nucleotides [10]. Mitochondrial Mg^{2+} constitutes one of the major cellular pools of this divalent cation, and currently reported in the mM concentration range in the mitochondrial matrix [11], most of which in complexed form [12]. Among the divalent cations which can replace Mg^{2+}, ~~such as~~ Ca^{2+}, which supports ATP hydrolysis but not ATP synthesis, has been especially investigated. Accordingly, mitochondrial calcium and magnesium concentrations are interrelated [13], and both cations are involved in enzyme activation and signaling in mitochondria [13,14]. Free calcium remains quite stable in the mitochondrial matrix in the range 1-5 μM, even if the cellular concentration increases. However, under certain conditions and in some cellular types, Ca^{2+} concentration can exceed 100μM in mitochondria [15]. The proton translocation capability of the Ca-driven F-ATPase activity is still controversial. In *Escherichia coli* CaATP was shown to drive the pH gradient formation with nearly the same effectiveness as MgATP [16]. However, in bacteria [17,18], chloroplasts [19] and beef heart submitochondrial particles [20], the Ca-dependent F-ATPase was reported as unable to translocate protons. Even if the Ca-dependent ATP hydrolysis is decoupled from proton pumping activity, the F_1F_O-ATPase mechanism of rotational catalysis is maintained [21]. Nowadays, it is ascertained that Ca^{2+} binds to the catalytic site of the F_1F_O-ATPase

dimeric form [22]. Such binding triggers still undefined conformational changes within the F_O domain, which in turn promote the permeability transition pore (PTP) formation [22,23]. The PTP formation is a deleterious event, which, other than causing an abrupt loss of osmotic homeostasis to small solutes, triggers signaling pathways which lead to cell death through different mechanisms [24]. Interestingly, increasing literature highlights the PTP involvement in a variety of human diseases, spanning from cardiovascular diseases to neurological disorders [25–27]. The PTP formation is hampered by F_1F_O-ATPase modulators (ATP, ADP and Mg^{2+}), but it is refractory to oligomycin [23], a specific F_1F_O-ATPase inhibitor [28]. Furthermore, the PTP formation is known to require neutral pH [29], while the pH dependence curve of the Mg-stimulated ATP hydrolysis mainly lies in the alkaline field. To sum up, present knowledge supports the idea that, if the F_1F_O-ATPase could be related to the PTP or even be part of it, even if this point is still a matter of debate, the Ca-dependent F-ATPase activity is unrelated to PTP opening [23]. The present study was designed to deepen the knowledge on the distinct enzyme kinetic features when activated by the natural cofactor Mg^{2+} or by Ca^{2+} [22] whose rise in concentration is usually linked to negative events in mitochondria [30–32].

2. Materials and Methods

2.1. Chemicals

Na_2ATP, NaADP, oligomycin mixture (A:B:C 64:15:17%), 1,4-Dithioerythritol (DTE), 2,5-Di-*tert*-butylhydroquinone (BHQ), Tributyltin (TBT), *N*,*N*′-dicyclohexylcarbodiimide (DCCD), 2,4-Dinitrophenol (DNP), sodium succinate (Succ), rotenone (ROT), atractyloside and sodium orthovanadate were obtained from Sigma–Aldrich (Milan, Italy). Thapsigargin and sodium azide (NaN_3) were purchased by Vinci-Biochem (Vinci, Italy). All other chemicals were reagent grade. Quartz double distilled water was used for all reagent solutions except when differently stated.

2.2. Preparation of the mitochondrial fractions

Swine hearts (*Sus scrofa domesticus*) were collected at a local abattoir and transported to the lab within 2 h in ice buckets at 0-4 °C. After removal of fat and blood clots as much as possible, approximately 30-40 g of heart tissue were rinsed in ice-cold washing Tris-HCl buffer (medium A) consisting of 0.25 M sucrose, 10 mM Tris(hydroxymethyl)-aminomethane (Tris), pH 7.4 and finely chopped into fine pieces with scissors. Each preparation was made from one heart. Once rinsed, tissues were gently dried on blotting paper and weighted. Then tissues were homogenized in the homogenizing buffer (medium B) consisting of 0.25 mM sucrose, 10 mM Tris, 1 mM EDTA (free

acid), 0.5 mg/mL BSA, pH 7.4 with HCl. After a preliminary gentle break up by Ultraturrax T25, the tissue was carefully homogenized by a motor-driven teflon pestle homogenizer (Braun Melsungen Type 853202) at 650 rpm with 3 up-and-down strokes. The mitochondrial fraction was then obtained by stepwise centrifugation (Sorvall RC2-B, rotor SS34). Briefly, the homogenate was centrifuged at 1,000 *g* for 5 min, thus yielding a supernatant and a pellet. The pellet was re-homogenized under the same conditions of the first homogenization and re-centrifuged at 1,000 *g* for 5 min. The gathered supernatants from these two centrifugations, filtered through four cotton gauze layers, were centrifuged at 10,500 *g* for 10 min to yield the raw mitochondrial pellet. The raw pellet was resuspended in medium A and further centrifuged at 10,500 *g* for 10 min to obtain the final mitochondrial pellet. The latter was resuspended by gentle stirring using a Teflon Potter Elvejehm homogenizer in a small volume of medium A, thus obtaining a protein concentration of 30 mg/mL. All steps were carried out at 0-4 °C. The protein concentration was determined according to the colorimetric method of Bradford [33] by Bio-Rad Protein Assay kit II with bovine serum albumin (BSA) as standard. The mitochondrial preparations were then stored in liquid nitrogen until the evaluation of ATPase activities.

2.3. Preparation of inside-out submitochondrial particles (IO-SMP)

Mitochondria were diluted with Tris–HCl buffer (medium C) containing 0.25 M sucrose, 2 mM EDTA, 10 mM Tris (pH 7.4) up to obtain a concentration of 20 mg/mL protein. The mitochondrial suspension in a vial was saturated with N_2 and subjected to sonic oscillation on ice with MSE Sonicator Soniprep 150 at 210 μm of amplitude for 5 times for 2 seconds with 10 seconds of intervals. The IO-SMP particles were isolated by stepwise centrifugation according to the method of Møller [34] with some modifications as follows. The sonicated preparations were diluited 1:2 with medium C and centrifuged at 16,000 *g* for 10 min at 4 °C. The supernatant obtained was further centrifuged at 150,000 *g* for 45 min at 4 °C. The pellet containing submitochondrial particles was carefully resuspended in the medium B and homogenized by gentle stirring using a Teflon Potter Elvejehm homogenizer. The protein concentration was determined according to the method of Bradford [33]. The IO-SMP were stored in liquid nitrogen. The presence of IO-SMP was ascertained by the stimulation of the ATPase activity by 100 μM DNP and by the failed inhibition (<5%) by 150 μM atractyloside [35].

2.4. Preincubation and treatment of mitochondria

In selected experiments, to favor incorporation of the compounds within the mitochondrial membranes and avoid the direct interference between different reagents, enzymatic assays were

carried out on mitochondria preincubated for 30 min on ice with the compounds to be tested. Accordingly, the preincubation of mitochondria with selected TBT doses aimed at ensuring TBT incorporation within the membranes and at evaluating the effect of the thiol reagent dithioerythritol (DTE), ruling out a direct interaction between DTE and TBT. In detail, mitochondria were preincubated with dimethylsulfoxide (DMSO) (control) or appropriate TBT amounts in DMSO to yield the final 30 μM TBT concentrations in the reaction system. To prevent possible chemical interactions between TBT and DTE, 100 μM DTE were added in the TBT-preincubated mitochondrial suspensions only when acclimated to 37 °C. After this incubation time, the F-ATPase reaction was carried out as described in the Section 2.5. The DTE concentrations employed were the same as previously tested [36].

2.5. Assay of the mitochondrial F-ATPase activity

Thawed mitochondrial fractions were immediately used for ATPase activity assays. Whenever a preincubation procedure was applied, immediately after the preincubation time, appropriate aliquots of the preincubated mitochondrial suspensions were sampled by a micropipette and directly added to the ATPase reaction media to yield the final concentration of 0.15 mg protein/mL.

The capability of ATP hydrolysis was assayed in a reaction medium (1 mL) containing 75 mM ethanolammine-HCl buffer pH 9.3, 0.15 mg mitochondrial protein plus 6.0 mM Na_2ATP and 2.0 mM $MgCl_2$ for the Mg-dependent F_1F_O-ATPase assay (hereafter defined as Mg-dependent F-ATPase), and ethanolammine-HCl buffer pH 9.0, 0.15 mg mitochondrial protein plus 3.0 mM Na_2ATP and 2.0 mM $CaCl_2$ for the Ca-dependent F_1F_O-ATPase assay (defined as Ca-dependent F-ATPase). After 5 min preincubation at 37 °C, the reaction, carried out at the same temperature, was started by the addition of the substrate ATP and stopped after 5 min by the addition of 1 mL of ice-cold 15% (w/w) aqueous solution trichloroacetic acid (TCA). Once the reaction was stopped, vials were centrifuged for 15 min at 5000 rpm (ALC 4225 Centrifuge). In the supernatant, the concentration of inorganic phosphate (P_i) hydrolyzed by known amounts of mitochondrial protein, which is an indirect measure of ATPase activity, was spectrophotometrically evaluated.

The ATPase activity was routinely measured by subtracting, from the P_i hydrolyzed by known amounts of mitochondrial protein (which indirectly indicates the total ATPase activity), the P_i hydrolyzed in the presence of 3 μg/mL oligomycin. To this aim, 1 μL from a mother solution of 3 mg/mL oligomycin in DMSO was directly added to the reaction mixture before starting the reaction. The total ATPase activity was calculated by detecting the P_i in control tubes run in parallel and containing 1 μL DMSO per mL reaction system. In each experimental set, control tubes were alternated to the condition to be tested. The employed dose of oligomycin, a specific inhibitor of F-

ATPases which selectively blocks the F_O subunit, ensured maximal enzyme activity inhibition and was currently used in ATPase assays [37]. In all the experiments the F-ATPase activity was calculated as μmoles P_i·mg protein^{-1}·min^{-1}.

2.6. Inhibition kinetics by DCCD

To obtain time-course plots the F-ATPase reaction was carried out in the presence of 5 μM DCCD, previously solubilized in DMSO (directly added with the ATP substrate) in the reaction system and stopped after different time intervals by TCA, namely from 1 to 20 min. Data were then plotted as percentages of the residual F-ATPase activity in the presence of 5 μM DCCD (θ) versus the DCCD incubation time. In this plot 100% F-ATPase activity corresponded to the initial enzyme activity (θ_i), assumed that DCCD is not bound to the enzyme [38]. By fitting the data in a semilogarithmic plot, straight lines were obtained according to the equation:

$$\log \theta = -\frac{k_{DCCD}}{2.3} t + \log \theta_i$$

The slope of each straight line corresponds to $-k_{DCCD}/2.3$ and the y-axis intercept to log θ_i. Thus, for the two divalent cations tested, the rate constant for DCCD inhibition (k_{DCCD}) was calculated from the slope (k_{DCCD}=slope·2.3·60^{-1}) and expressed as ms^{-1}. When θ is ½θ_i, t represents the "halflife" ($t_{1/2}$) of the inhibitor, namely it corresponds to a condition in which half of the number of inhibitor molecules originally present in the reaction system are bound to the enzyme [38,39].

2.7. Kinetic analyses

To calculate the kinetic parameters (V_{max} and K_m) in the presence and in the absence of inhibitors, enzyme activity data were fitted to the Lineweaver-Burk equation.

To detect the inhibition type and obtain the values of K_i and K'_i respectively, the mechanism of the enzyme inhibition by ADP and azide were explored by the aid of the graphical methods of Dixon and Cornish-Bowden, which complement one another [40]. In all kinetic analyses, the enzyme specific activity was taken as the expression of the reaction rate (v). The correlation coefficients of all the straight lines obtained in Lineweaver-Burk, Dixon and Cornish Bowden plots were never lower than 0.95, thus confirming the linearity of these plots [41]. At least three independent experiments were carried out to build each plot.

2.8. Statistical analyses

All differences between control and treated values were evaluated by one way ANOVA followed by Students-Newman-Keuls' test or Bonferroni's test when F values indicated significance ($P \leq 0.05$). Percentage data were arcsin transformed prior to statistical analysis to ensure normality.

3. Results and Discussion

3.1. Properties of F_O domain of the Ca-dependent F-ATPase activity

A crucial point of this work was to verify if the Ca-dependent F-ATPase activity maintains the F_1F_O-ATPase properties shown when activated by Mg^{2+} or not. Different divalent cations can sustain ATP hydrolysis by the enzyme [20,42] even if not all cations maintain the coupled H^+ pumping activity. On the other hand, the coupling efficiency of V-pump in the presence of Ca^{2+} driving the proton pump was shown to be modulated by membrane potential [43]. On these bases, our experiments using IO-SMP aimed at evaluating the Ca- and Mg-dependent F-ATPase activity dependence on Δp. In detail, the F_1F_O-ATPase translocates H^+ in the lumen of IO-SMP to build Δp and any increase in Δp indirectly contrasts and lessens the F-ATPase activity. In this scenario, the protonophore DNP dissipates Δp and increases the F_1F_O-ATPase activity. In contrast, if succinate plus rotenone (Succ+ROT) is added to stimulate the H^+ pumping activity of respiratory complexes, the Δp building counteracts the F_1F_O-ATPase activity. As shown in Figure 1, both the Ca- and Mg-dependent F-ATPase are increased by DNP and inhibited by Succ+ROT, thus they are similarly modulated by Δp. The maintenance in IO-SMP of the F_1F_O-ATPase capability of translocating protons irrespective of the cofactor divalent cation, contrasts with previous reports that the rotation driven by ATP hydrolysis stimulated by Ca^{2+} [21] is not coupled to H^+ translocation [17–20].

Interestingly, under non-physiological conditions, the F_1F_O-ATPase can show an uncoupled proton leakage known as "proton slip" [44]. In this case, protons (H^+) flow across F_O in the absence of nucleotides bound to F_1. On the basis of the results, we can hypothesize that the Ca-dependent F-ATPase would perform an "uncoupled ATP hydrolysis", namely a sort of "inverse-slip". When F_1 is linked to F_O, the inhibition of H^+ pumping by oligomycin is directly accompanied by the suppression of catalysis by F_1 [28,45]. As known, the so-called "proton slip" is abolished by F_O inhibitors, but it is insensitive to F_1 inhibitors [44]. Therefore, we can reasonably assume that the Ca-dependent F-ATPase can be insensitive to inhibitors that specifically block H^+ translocation such as DCCD and oligomycin. In hydrophobic environment DCCD irreversibly establishes a covalent bound with the *c* subunit carboxylic groups of H^+ binding site and prevents H^+ translocation [46]. To explore this point, the effect of oligomycin and DCCD was evaluated in parallel on both the Ca- and Mg-dependent F-ATPases. When tested in the 7.0 – 10.5 pH range,

DCCD maximally inhibited (92%) the Ca-dependent F-ATPase approximately at pH 9.0, while it almost completely inhibited (100%) the Mg-dependent F-ATPase at any pH tested (Fig. 2A). In addition, the residual F-ATPase activity (*offset*) detected after 20 min of DCCD incubation (Fig. 2B), was the same in the presence of Ca^{2+} or Mg^{2+} (Table 1). Furthermore, since the Ca-dependent F-ATPase showed greater K_{DCCD} and lower $t_{½}$ than the Mg-dependent F-ATPase (Table 1), it seems clear that the former more promptly reacts and binds DCCD than the latter. Probably, the conserved Ca^{2+} binding site formed by Asp residues in the N-terminal region of *c* subunits [47] could favor DCCD binding, according to a well established model [46] and/or Ca^{2+} insertion may increase the hydrofobicity of the H^+ binding site of *c*-ring [48]. Moreover, both the Ca- and Mg-dependent F-ATPases showed a similar bell-shaped pH profile (Fig. 2D), which is typical of F_1F_O-ATPases which translocate H^+ by coordinating the hydronium ion (H_3O^+) in the proton binding site of F_O [38,49]. Consequently, these findings suggest that, when activated by Ca^{2+}, the F_1F_O-ATPase maintains the proton binding capability within F_O by the same mechanism as the Mg-dependent F-ATPase.

The structural identity of the Ca-dependent F-ATPase was also checked by testing the responsiveness to a variety of selective inhibitors: vanadate (inhibitor P type ATPases) [50]; thapsigargin (inhibitor sarco-endoplasmic reticulum Ca-ATPase) [51]; butylhydroquinone (inhibitor of sarcoplasmic reticulum Ca-ATPase) [52]; oligomycin (inhibitor of F_O sector F-ATPase) [45]. The results show that both the Ca- and Mg-dependent F-ATPases were only inhibited by oligomycin (Table 2), thus ruling out the possibility that the detected ATPase activities mirror other ATP consuming reactions in the mitochondrial preparations. Moreover, the oligomycin sensitivity indicates that with both Ca^{2+} or Mg^{2+} as cofactor the coupling between the proton-driven motor F_O and the ATP-driven motor F_1 is maintained [45]. Other experiments (Figure 3) pointed out that, the reversible loss of sensitivity to oligomycin produced by thiol oxidation, which is a peculiar property of the mitochondrial Mg-dependent F-ATPase [36,37], is shared by the Ca-dependent F-ATPase. Accordingly, in both cases, the enzyme activity was nearly suppressed by 3 μg/mL oligomycin, but the inhibition was removed by TBT. Interestingly, the combination of TBT, oligomycin and the thiol reagent DTE, in which DTE strongly limits the free thiol availability, made TBT ineffective in this respect, resulting into a nearly complete enzyme inhibition both of the Ca-dependent and the Mg-dependent F-ATPases (Fig. 3). These findings can be interpreted on the basis of previous data. It is well known that oligomycin covers the *c*-ring binding sites of by interacting with two adjacent *c* subunits [53], thus blocking H^+ translocation. Since such inhibition is removed when conserved Cys in the C-terminal α-helix of *c* subunit [54] are oxidized by reversible TBT binding [36], we can infer that the two F-ATPase activities share the same structural properties of F_O domain.

Taken together, all these experiments did not elicit any significant difference between the Ca- and Mg-dependent F-ATPase features. Therefore, the commonalities pointed out indicate that, most likely, the torque generation driven by ATPase activity in presence of Ca^{2+} cofactor ensures H^+ translocation as in the case of the classical Mg-dependent F-ATPase.

3.2. Ca^{2+} and Mg^{2+} efficiency in the enzyme catalysis

Kinetic analyses can help to understand the ATP hydrolysis mechanism in the presence of different cations, which act as cofactors. Ca^{2+} and Mg^{2+} play a complex interplay in mitochondria [13] and their concentrations in the mitochondrial matrix are not only interconnected but also tightly related to the transmembrane potential [13,15]. Previous studies in our lab pointed out that the Mg-dependent F-ATPase activity is apparently more efficient than the Ca-dependent F-ATPase ~~latter~~. In detail, the V_{max} attains threefold higher values in the case of the Mg-dependent F-ATPase (2.87 *vs* 0.85 μmol P_i mg $protein^{-1}$ min^{-1}), while the K_m value of the Mg-dependent F-ATPase is about one fifth of that of the Ca-dependent F-ATPase (0.12 *vs* 0.62 mM) [55]. In the present study we tried to obtain further information on the kinetic mechanisms involved by evaluating the inhibition mechanism of ADP. It is known that when ADP remains bound to the *β* subunit catalytic sites, ATP cannot be hydrolyzed and the MgADP-inhibited F_1 structure represents a "transition state" intermediate in ATP hydrolysis [56]. ADP acts as competitive inhibitor of the Mg-dependent F-ATPase [57] and competitive inhibition implies a different mechanism from the mixed type inhibition pointed out for the Ca-dependent F-ATPase (Fig. 4 A,B). As defined by the term "competitive", in the case of the Mg-dependent F-ATPase, the inhibitor ADP competes with the ATP substrate for the free enzyme. On the other hand, the mixed-type inhibition mechanism implies that the inhibitor can also bind to the enzyme-substrate complex. To cast light on which is the preferred complex, the dissociation constants of these two complexes were calculated. In kinetic terms, K_i refers to the dissociation constant of the enzyme-inhibitor complex, namely the enzyme-ADP complex, while K'_i is the dissociation constant of the tertiary complex enzyme-ATP-ADP. In the presence of Ca^{2+} the resulting $K_i < K'_i$, clearly indicates that the formation of the binary complex (enzyme-ADP) is favored with respect to the tertiary complex (enzyme-ATP-ADP). As a rule, the Mg-dependent F-ATPase activity involves the MgADP trapping in the catalytic sites β_{TP}, β_{DP}, and β_E. The β_E conformation adopts a "half-closed" conformation with bound MgADP [56]. The inhibition by ADP is removed when ATP binds to the non-catalytic sites (*α* subunits). It should be stressed that ATP binding, which only occurs in the closed conformation, is not required to synthesize ATP [58], but only to detach ADP from the β sites. Consequently, the F_1F_O-ATPase only hydrolyzes ATP when ADP is not bound.

To explore what happens in the presence of Ca^{2+}, the inhibitor azide, known to act as non-competitive inhibitor on the F-ATPase activity with respect to MgATP [59], was tested. From these experiments, the plots drawn in Figure 4 C,D were obtained, which clearly indicate a mixed-type inhibition mechanism on the Ca-dependent F-ATPase, namely the inhibitor azide can bind either to the free enzyme or to the enzyme-ATP complex. Interestingly, azide binds to the Ca-dependent F-ATPase with nearly doubled affinity (halved K_i) in the presence of ATP (enzyme-ATP complex) than in its absence (K_i =71.0 μM versus K'_i =140.0 μM). Previous studies on the azide inhibition mechanism [60] indicate that the $\alpha_3\beta_3$-ADP complex can bind azide to yield the $\alpha_3\beta_3$-(ADP-azide) complex, in which both ADP and azide are bound to the β subunit. Moreover ADP binding increases the enzyme sensitivity to azide [59]. Consistently, also in the case of the Ca-dependent F-ATPase, ADP enhanced the enzyme inhibition by azide and in parallel increased the K_m value, namely ADP decreased the enzyme affinity for the substrate ATP (Figure 4E). These data confirm that the inhibitor azide tightly binds to the enzyme complex only if ADP and Mg^{2+} are already bound [61] and in the same way, when Ca^{2+} replaces Mg^{2+}, only if ADP and Ca^{2+} are already bound. To sum up, it seems that the enzyme catalytic properties are independent of the cofactor cation. However, some clues combined with literature reports suggest that the catalytic mechanism within F_1 may be cation-dependent. In detail, during ATP hydrolysis the F_1F_O-ATPase catalytic sites may adopt different conformations if Ca^{2+} or Mg^{2+} are bound. Figure 5 illustrates the β_{DP} sites occupied by MgATP (A,B) and CaATP (C,D), according to our hypothesis. The adenosine moiety is sandwiched between $_{\beta}Tyr^{345}$ and $_{\beta}Phe^{424}$. The Walker motif or P-loop establishes an electrostatic interaction with the phosphate groups of ATP. Only the $_{\beta}Thr^{163}$ of P-loop is directly linked to Mg^{2+}. To complete the coordination bonds with Mg^{2+} three water molecules build a bridge interaction between the cation and the $_{\beta}Arg^{189}$, $_{\beta}Glu^{192}$, $_{\beta}Asp^{256}$ residues. The remaining two bonds with Mg^{2+}, as well as with all divalent cations, would involve the phosphate oxygens of ATP or ADP. The binding pocket is formed by the P-loop and $_{\alpha}Arg^{373}$, which allows the allocation of the γ-phosphate in the β_{TP} conformation [4]. Previous studies on mutants in which $_{\beta}Thr^{163}$ was substituted by other aminoacids [18] suggest that the β subunit adopts different conformational states when Ca^{2+}, which implies a higher steric hindrance, replaces Mg^{2+} in the catalytic site [18]. The ion coordination geometry within the F_1 sector would change since Mg^{2+} always onsets hexacoordinated octahedral complexes, while Ca^{2+} coordinates up to eight bonds. Therefore, the rigid octahedral complex would change into a less rigid geometry resulting into irregular bond distances, variable coordination number and bond angles [62]. Moreover, the α-subunit can only bind MgATP, while the β-subunit can bind both Mg^{2+} and Ca^{2+}, in turn electrostatically bound to adenine nucleotides [63]. On the other hand, if the F_1F_O complex cannot synthesize ATP in presence of Ca^{2+} as cofactor,

it may regulate its ATPase activity through the *e* subunit, which, consistently, contains an aminoacid sequence similar to the Ca^{2+}-dependent tropomyosin binding region of troponin T [64].

4. Conclusion

Many hints emerge from these findings. To sum up, even if the Ca-dependent F-ATPase has up to now been not considered an H^+-translocating enzyme, the evidence here collected suggests that it can translocate protons. Further studies on the F_1F_O-ATPase driven by Ca^{2+} are required to shed light on its putative involvement in the complex event of PTP opening.

The whole of data sustain the idea that the Ca-dependent and Mg-dependent F-ATPase activities are two distinct functioning modes of the same F_1F_O mitochondrial complex. As a matter of fact, most properties are shared by the Ca-dependent and Mg-dependent F-ATPase activities, while others, which strictly refer to the intimate mechanism of F_1 catalysis or to the features of the proton binding site of F_O, appear to be cation-sensitive. These differences and others, which hopefully can be unraveled in the next future, are probably the key of the *in vivo* role of the Ca-dependent F-ATPase.

The role of calcium in mitochondria is increasingly coming out. In cardiomyocytes, matrix calcium increases under conditions of increased work with the putative task to modulate the activity of mitochondrial enzymes [15]. It is intriguing to speculate that the enlightenment of the features of the Ca-activated mitochondrial enzyme and of its responsiveness to chemical modulators may be exploited to address the cell fate.

5. Conflict of interest

None

6. Acknowledgements

Danilo Matteuzzi (Department of Veterinary Medical Sciences, University of Bologna) is gratefully acknowledged for kindly conferring swine hearts from a local abattoir to our lab.

This work was financed by a RFO grant from the University of Bologna, Italy.

7. References

[1] W. Junge, N. Nelson, ATP synthase, Annu. Rev. Biochem. 84 (2015) 631–657. doi:10.1146/annurev-biochem-060614-034124.

[2] P.D. Boyer, The ATP synthase--a splendid molecular machine, Annu. Rev. Biochem. 66 (1997) 717–749. doi:10.1146/annurev.biochem.66.1.717.
[3] J.E. Walker, The ATP synthase: the understood, the uncertain and the unknown, Biochem. Soc. Trans. 41 (2013) 1–16. doi:10.1042/BST20110773.
[4] J.P. Abrahams, A.G. Leslie, R. Lutter, J.E. Walker, Structure at 2.8 A resolution of F1-ATPase from bovine heart mitochondria, Nature. 370 (1994) 621–628. doi:10.1038/370621a0.
[5] J.E. Walker, V.K. Dickson, The peripheral stalk of the mitochondrial ATP synthase, Biochim. Biophys. Acta. 1757 (2006) 286–296. doi:10.1016/j.bbabio.2006.01.001.
[6] M. Allegretti, N. Klusch, D.J. Mills, J. Vonck, W. Kühlbrandt, K.M. Davies, Horizontal membrane-intrinsic α-helices in the stator a-subunit of an F-type ATP synthase, Nature. 521 (2015) 237–240. doi:10.1038/nature14185.
[7] S. Nesci, F. Trombetti, V. Ventrella, A. Pagliarani, Opposite rotation directions in the synthesis and hydrolysis of ATP by the ATP synthase: hints from a subunit asymmetry, J. Membr. Biol. 248 (2015) 163–169. doi:10.1007/s00232-014-9760-y.
[8] D. Pogoryelov, O. Yildiz, J.D. Faraldo-Gómez, T. Meier, High-resolution structure of the rotor ring of a proton-dependent ATP synthase, Nat. Struct. Mol. Biol. 16 (2009) 1068–1073. doi:10.1038/nsmb.1678.
[9] P.D. Boyer, Catalytic site occupancy during ATP synthase catalysis, FEBS Lett. 512 (2002) 29–32.
[10] W.D. Frasch, The participation of metals in the mechanism of the F(1)-ATPase, Biochim. Biophys. Acta. 1458 (2000) 310–325.
[11] D.W. Jung, C.J. Chapman, K. Baysal, D.R. Pfeiffer, G.P. Brierley, On the use of fluorescent probes to estimate free Mg2+ in the matrix of heart mitochondria, Arch. Biochem. Biophys. 332 (1996) 19–29. doi:10.1006/abbi.1996.0311.
[12] E. Gout, F. Rébeillé, R. Douce, R. Bligny, Interplay of Mg2+, ADP, and ATP in the cytosol and mitochondria: unravelling the role of Mg2+ in cell respiration, Proc. Natl. Acad. Sci. U. S. A. 111 (2014) E4560-4567. doi:10.1073/pnas.1406251111.
[13] T. Kubota, Y. Shindo, K. Tokuno, H. Komatsu, H. Ogawa, S. Kudo, Y. Kitamura, K. Suzuki, K. Oka, Mitochondria are intracellular magnesium stores: investigation by simultaneous fluorescent imagings in PC12 cells, Biochim. Biophys. Acta. 1744 (2005) 19–28. doi:10.1016/j.bbamcr.2004.10.013.
[14] R. Rizzuto, D. De Stefani, A. Raffaello, C. Mammucari, Mitochondria as sensors and regulators of calcium signalling, Nat. Rev. Mol. Cell Biol. 13 (2012) 566–578. doi:10.1038/nrm3412.
[15] T. Finkel, S. Menazza, K.M. Holmström, R.J. Parks, J. Liu, J. Sun, J. Liu, X. Pan, E. Murphy, The ins and outs of mitochondrial calcium, Circ. Res. 116 (2015) 1810–1819. doi:10.1161/CIRCRESAHA.116.305484.
[16] D.S. Perlin, L.R. Latchney, J.G. Wise, A.E. Senior, Specificity of the proton adenosinetriphosphatase of Escherichia coli for adenine, guanine, and inosine nucleotides in catalysis and binding, Biochemistry (Mosc.). 23 (1984) 4998–5003.
[17] Z. Gromet-Elhanan, S. Weiss, Regulation of .DELTA.~.mu.H + -coupled ATP synthesis and hydrolysis: role of divalent cations and of the F0F1-.beta. subunit, Biochemistry (Mosc.). 28 (1989) 3645–3650. doi:10.1021/bi00435a004.
[18] L. Nathanson, Z. Gromet-Elhanan, Mutations in the β-subunit Thr159 and Glu184 of the Rhodospirillum rubrum F0F1 ATP synthase reveal differences in ligands for the coupled Mg2+- and decoupled Ca2+-dependent F0F1 activities, J. Biol. Chem. 275 (2000) 901–905. doi:10.1074/jbc.275.2.901.
[19] U. Pick, M. Weiss, A light-dependent dicyclohexylcarbodiimide-sensitive Ca-ATPase activity in chloroplasts which is not coupled to proton translocation, Eur. J. Biochem. 173 (1988) 623–628.
[20] S. Papageorgiou, A.B. Melandri, G. Solaini, Relevance of divalent cations to ATP-driven proton pumping in beef heart mitochondrial F0F1-ATPase, J. Bioenerg. Biomembr. 30 (1998) 533–541.
[21] W.C. Tucker, A. Schwarz, T. Levine, Z. Du, Z. Gromet-Elhanan, M.L. Richter, G. Haran, Observation of calcium-dependent unidirectional rotational motion in recombinant photosynthetic F1-ATPase molecules, J. Biol. Chem. 279 (2004) 47415–47418. doi:10.1074/jbc.C400269200.

[22] V. Giorgio, V. Burchell, M. Schiavone, C. Bassot, G. Minervini, V. Petronilli, F. Argenton, M. Forte, S. Tosatto, G. Lippe, P. Bernardi, Ca(2+) binding to F-ATP synthase β subunit triggers the mitochondrial permeability transition, EMBO Rep. (2017). doi:10.15252/embr.201643354.

[23] P. Bernardi, A. Rasola, M. Forte, G. Lippe, The Mitochondrial Permeability Transition Pore: Channel Formation by F-ATP Synthase, Integration in Signal Transduction, and Role in Pathophysiology, Physiol. Rev. 95 (2015) 1111–1155. doi:10.1152/physrev.00001.2015.

[24] V. Izzo, J.M. Bravo-San Pedro, V. Sica, G. Kroemer, L. Galluzzi, Mitochondrial Permeability Transition: New Findings and Persisting Uncertainties, Trends Cell Biol. 26 (2016) 655–667. doi:10.1016/j.tcb.2016.04.006.

[25] M.S. Arrázola, E. Ramos-Fernández, P. Cisternas, D. Ordenes, N.C. Inestrosa, Wnt Signaling Prevents the Aβ Oligomer-Induced Mitochondrial Permeability Transition Pore Opening Preserving Mitochondrial Structure in Hippocampal Neurons, PloS One. 12 (2017) e0168840. doi:10.1371/journal.pone.0168840.

[26] S. Nesci, V. Ventrella, F. Trombetti, M. Pirini, A. Pagliarani, Mini-review. Nitrite as novel pore-shutter: hints from the preferential inhibition of the mitochondrial ATP-ase when activated by Ca2+, Sci. E Ric. 44 (2017) 57–63.

[27] M.Z. Rasheed, H. Tabassum, S. Parvez, Mitochondrial permeability transition pore: a promising target for the treatment of Parkinson's disease, Protoplasma. 254 (2017) 33–42. doi:10.1007/s00709-015-0930-2.

[28] A. Pagliarani, S. Nesci, V. Ventrella, Modifiers of the oligomycin sensitivity of the mitochondrial F1F0-ATPase, Mitochondrion. 13 (2013) 312–319. doi:10.1016/j.mito.2013.04.005.

[29] A. Nicolli, V. Petronilli, P. Bernardi, Modulation of the mitochondrial cyclosporin A-sensitive permeability transition pore by matrix pH. Evidence that the pore open-closed probability is regulated by reversible histidine protonation, Biochemistry (Mosc.). 32 (1993) 4461–4465.

[30] V. Giorgio, S. von Stockum, M. Antoniel, A. Fabbro, F. Fogolari, M. Forte, G.D. Glick, V. Petronilli, M. Zoratti, I. Szabó, G. Lippe, P. Bernardi, Dimers of mitochondrial ATP synthase form the permeability transition pore, Proc. Natl. Acad. Sci. U. S. A. 110 (2013) 5887–5892. doi:10.1073/pnas.1217823110.

[31] L. Biasutto, M. Azzolini, I. Szabò, M. Zoratti, The mitochondrial permeability transition pore in AD 2016: An update, Biochim. Biophys. Acta. 1863 (2016) 2515–2530. doi:10.1016/j.bbamcr.2016.02.012.

[32] G. Beutner, K.N. Alavian, E.A. Jonas, G.A. Porter, The Mitochondrial Permeability Transition Pore and ATP Synthase, Handb. Exp. Pharmacol. (2016). doi:10.1007/164_2016_5.

[33] M.M. Bradford, A rapid and sensitive method for the quantitation of microgram quantities of protein utilizing the principle of protein-dye binding, Anal. Biochem. 72 (1976) 248–254.

[34] I.M. Møller, A.C. Lidén, I. Ericson, P. Gardeström, [41] Isolation of submitochondrial particles with different polarities, Methods Enzymol. 148 (1987) 442–453. doi:10.1016/0076-6879(87)48043-9.

[35] S. Nesci, V. Ventrella, F. Trombetti, M. Pirini, A. Pagliarani, Tri-n-butyltin binding to a low-affinity site decreases the F 1F O-ATPase sensitivity to oligomycin in mussel mitochondria, Appl. Organomet. Chem. 26 (2012) 593–599. doi:10.1002/aoc.2904.

[36] S. Nesci, V. Ventrella, F. Trombetti, M. Pirini, A. Pagliarani, The mitochondrial F1FO-ATPase desensitization to oligomycin by tributyltin is due to thiol oxidation, Biochimie. 97 (2014) 128–137. doi:10.1016/j.biochi.2013.10.002.

[37] S. Nesci, V. Ventrella, F. Trombetti, M. Pirini, A. Pagliarani, Thiol oxidation is crucial in the desensitization of the mitochondrial F1FO-ATPase to oligomycin and other macrolide antibiotics, Biochim. Biophys. Acta. 1840 (2014) 1882–1891. doi:10.1016/j.bbagen.2014.01.008.

[38] S. Nesci, V. Ventrella, F. Trombetti, M. Pirini, A. Pagliarani, Mussel and mammalian ATP synthase share the same bioenergetic cost of ATP, J. Bioenerg. Biomembr. 45 (2013) 289–300. doi:10.1007/s10863-013-9504-1.

[39] K. Mizutani, M. Yamamoto, K. Suzuki, I. Yamato, Y. Kakinuma, M. Shirouzu, J.E. Walker, S. Yokoyama, S. Iwata, T. Murata, Structure of the rotor ring modified with N,N'-dicyclohexylcarbodiimide of the Na+-transporting vacuolar ATPase, Proc. Natl. Acad. Sci. U. S. A. 108 (2011) 13474–13479. doi:10.1073/pnas.1103287108.

[40] A. Cornish-Bowden, A simple graphical method for determining the inhibition constants of mixed, uncompetitive and non-competitive inhibitors, Biochem. J. 137 (1974) 143–144.

[41] S. Nesci, V. Ventrella, F. Trombetti, M. Pirini, A.R. Borgatti, A. Pagliarani, Tributyltin (TBT) and dibutyltin (DBT) differently inhibit the mitochondrial Mg-ATPase activity in mussel digestive gland, Toxicol. Vitro Int. J. Publ. Assoc. BIBRA. 25 (2011) 117–124. doi:10.1016/j.tiv.2010.10.001.
[42] N. Williams, J. Hullihen, P.L. Pedersen, Mitochondrial ATP synthase: role of metal binding in structure and function, Prog. Clin. Biol. Res. 273 (1988) 87–92.
[43] B.P. Crider, X.-S. Xie, Characterization of the functional coupling of bovine brain vacuolar-type H(+)-translocating ATPase. Effect of divalent cations, phospholipids, and subunit H (SFD), J. Biol. Chem. 278 (2003) 44281–44288. doi:10.1074/jbc.M307372200.
[44] B.A. Feniouk, A.Y. Mulkidjanian, W. Junge, Proton slip in the ATP synthase of Rhodobacter capsulatus: induction, proton conduction, and nucleotide dependence, Biochim. Biophys. Acta. 1706 (2005) 184–194. doi:10.1016/j.bbabio.2004.10.010.
[45] R.J. Devenish, M. Prescott, G.M. Boyle, P. Nagley, The Oligomycin Axis of Mitochondrial ATP Synthase: OSCP and the Proton Channel, J. Bioenerg. Biomembr. 32 (2000) 507–515. doi:10.1023/A:1005621125812.
[46] M.D. Partis, E. Bertoli, D.E. Griffiths, A. Azzi, Interaction of the dibutylchloromethyltin chloride binding site with the carbodiimide binding site in mitochondria, Biochem. Biophys. Res. Commun. 96 (1980) 1103–1108.
[47] T. Azarashvili, I. Odinokova, A. Bakunts, V. Ternovsky, O. Krestinina, J. Tyynelä, N.-E.L. Saris, Potential role of subunit c of F0F1-ATPase and subunit c of storage body in the mitochondrial permeability transition. Effect of the phosphorylation status of subunit c on pore opening, Cell Calcium. 55 (2014) 69–77. doi:10.1016/j.ceca.2013.12.002.
[48] S. Nesci, V. Ventrella, F. Trombetti, M. Pirini, A. Pagliarani, Tributyltin-driven enhancement of the DCCD insensitive Mg-ATPase activity in mussel digestive gland mitochondria, Biochimie. 94 (2012) 727–733. doi:10.1016/j.biochi.2011.11.002.
[49] C. von Ballmoos, P. Dimroth, Two distinct proton binding sites in the ATP synthase family, Biochemistry (Mosc.). 46 (2007) 11800–11809. doi:10.1021/bi701083v.
[50] M. Aureliano, G. Fraqueza, C.A. Ohlin, Ion pumps as biological targets for decavanadate, Dalton Trans. Camb. Engl. 2003. 42 (2013) 11770–11777. doi:10.1039/c3dt50462j.
[51] J. Lytton, M. Westlin, M.R. Hanley, Thapsigargin inhibits the sarcoplasmic or endoplasmic reticulum Ca-ATPase family of calcium pumps, J. Biol. Chem. 266 (1991) 17067–17071.
[52] A.A. Kabbara, D.G. Stephenson, Effects of 2,5-di-tert-butylhydroquinone on rat cardiac muscle contractility, Am. J. Physiol. - Heart Circ. Physiol. 272 (1997) H1001–H1010.
[53] J. Symersky, D. Osowski, D.E. Walters, D.M. Mueller, Oligomycin frames a common drug-binding site in the ATP synthase, Proc. Natl. Acad. Sci. U. S. A. 109 (2012) 13961–13965. doi:10.1073/pnas.1207912109.
[54] S. Nesci, V. Ventrella, F. Trombetti, M. Pirini, A. Pagliarani, Thiol oxidation of mitochondrial FO-c subunits: A way to switch off antimicrobial drug targets of the mitochondrial ATP synthase, Med. Hypotheses. 83 (2014) 160–165. doi:10.1016/j.mehy.2014.05.004.
[55] S. Nesci, V. Ventrella, F. Trombetti, M. Pirini, A. Pagliarani, Preferential nitrite inhibition of the mitochondrial F1FO-ATPase activities when activated by Ca(2+) in replacement of the natural cofactor Mg(2+), Biochim. Biophys. Acta. 1860 (2016) 345–353. doi:10.1016/j.bbagen.2015.11.004.
[56] R.I. Menz, J.E. Walker, A.G. Leslie, Structure of bovine mitochondrial F(1)-ATPase with nucleotide bound to all three catalytic sites: implications for the mechanism of rotary catalysis, Cell. 106 (2001) 331–341.
[57] D. Bald, T. Amano, E. Muneyuki, B. Pitard, J.L. Rigaud, J. Kruip, T. Hisabori, M. Yoshida, M. Shibata, ATP synthesis by F0F1-ATP synthase independent of noncatalytic nucleotide binding sites and insensitive to azide inhibition, J. Biol. Chem. 273 (1998) 865–870.
[58] J. Weber, C. Bowman, S. Wilke-Mounts, A.E. Senior, alpha-Aspartate 261 is a key residue in noncatalytic sites of Escherichia coli F1-ATPase, J. Biol. Chem. 270 (1995) 21045–21049.
[59] P. Mitchell, J. Moyle, Activation and inhibition of mitochondrial adenosine triphosphatase by various anions and other agents, J. Bioenerg. 2 (1971) 1–11.

[60] E. Muneyuki, M. Makino, H. Kamata, Y. Kagawa, M. Yoshida, H. Hirata, Inhibitory effect of NaN3 on the F0F1 ATPase of submitochondrial particles as related to nucleotide binding, Biochim. Biophys. Acta. 1144 (1993) 62–68.
[61] M.B. Murataliev, Y.M. Milgrom, P.D. Boyer, Characteristics of the combination of inhibitory Mg2+ and azide with the F1 ATPase from chloroplasts, Biochemistry (Mosc.). 30 (1991) 8305–8310.
[62] R. Casadio, B.A. Melandri, CaATP inhibition of the MgATP-dependent proton pump (H+-ATPase) in bacterial photosynthetic membranes with a mechanism of alternative substrate inhibition, J. Biol. Inorg. Chem. 1 (1996) 284–291.
[63] M.J. Hubbard, N.J. McHugh, Mitochondrial ATP synthase F1-beta-subunit is a calcium-binding protein, FEBS Lett. 391 (1996) 323–329.
[64] N. Arakaki, Y. Ueyama, M. Hirose, T. Himeda, H. Shibata, S. Futaki, K. Kitagawa, T. Higuti, Stoichiometry of subunit e in rat liver mitochondrial H(+)-ATP synthase and membrane topology of its putative Ca(2+)-dependent regulatory region, Biochim. Biophys. Acta. 1504 (2001) 220–228.
[65] M.W. Bowler, M.G. Montgomery, A.G.W. Leslie, J.E. Walker, Ground state structure of F1-ATPase from bovine heart mitochondria at 1.9 A resolution, J. Biol. Chem. 282 (2007) 14238–14242. doi:10.1074/jbc.M700203200.

Captions to Figures

Figure 1. Effect of Δp on the Ca- and Mg-dependent F-ATPase activities in IO-SMP. The Ca- (*A*) and Mg-dependent (*B*) F-ATPase activities were assayed in the presence of 100 μM dinitrophenol (DNP) or 5 mM succinate plus 1 μg/ml rotenone (Succ+ROT) and expressed as % of the enzyme activity detected in the absence of DNP, Succ and ROT. The control activity is 0.52±0.03 and 2.39±0.07 μmoles·P_i·mg protein^{-1}·min^{-1} for Ca and Mg-dependent F-ATPase respectively. The histograms represent the mean ± SD (vertical bars) of three distinct experiments. * indicate significantly different values ($P \leq 0.05$).

Figure 2. DCCD inhibition mechanism of the Ca- (○) and Mg-dependent (●) F-ATPase activities. pH dependence of the enzyme inhibition by 5 μM DCCD (*A*). The enzyme activities are expressed as percentage of the F-ATPase activity in the absence of DCCD; Time-course plots (*B*). The enzyme activities are expressed as percentage of the enzyme activity in the absence of DCCD (θ); Semilogarithmic plot of the DCCD inhibition kinetics (*C*), from which the parameters reported in Table 1 were obtained; pH dependence of the ATPase activities in the absence of DCCD (*D*). In (*A*, *B*, *C*) 5 μM DCCD was tested. In all graphs each point represents the mean value ± SD (vertical bars) of three experiments carried out on distinct pools.

Figure 3. Oligomycin sensitivity of the Ca- and Mg-dependent F-ATPase under different experimental conditions. The F-ATPase activity was evaluated in mitochondria as described in Section 2.4. In detail, 3 μg/ml oligomycin (olig), 100 μM DTE, 30 μM TBT were tested. Data are the mean ± SD (vertical bars) of three experiments carried out on different mitochondrial preparations. Different letters indicate significantly different values ($P \leq 0.05$).

Figure 4. Inhibition mechanisms of the Ca-dependent F-ATPase by ADP (*A*, *B*), azide (*C*, *D*) and by a binary mixture of both effectors (*E*). Dixon (*A*, *C*), Cornish-Bowden (*B*, *D*) and Lineweaver-Burk (*E*) plots were built as reported in Section 2.7. All points represent the mean ± SD (vertical bars) of tree distinct experiments carried out on distinct pools.

Figure 5. Illustration of a possible arrangement of the ground-state structure of F_1-ATPase [65] accommodating Mg^{2+} or Ca^{2+} in the β_{DP}-subunit. PDB ID code: 2JDI. The interactions of MgATP (Mg^{2+} as turquoise sphere) (*A* and *B*) or CaATP (Ca^{2+} as purple sphere) (*C* and *D*) in the β_{DP}-subunits are shown. MgATP or CaATP are bound to the catalytic site, the β subunit is represented as ribbon within F_1 (*A* and *C*). The position of key aminoacid residues in the β_{DP}-subunit that bind

ATP in presence of Mg^{2+} (*B*) or Ca^{2+} (*D*) is shown. The electron-density map of Mg^{2+} and Ca^{2+} is drawn as a sphere. The adenine ring of ATP, represented as ball and stick model, is inserted in the hydrophobic sandwich formed by $_{\beta}Phe^{424}$ and $_{\beta}Tyr^{345}$ (both in yellow wire frame). The Walker motif is highlighted in green and the aminoacid side chains are represented as wire frame. The $_{\beta}Thr^{163}$ side chain (pink) directly interacts by electrostatic bonds with the divalent cation, while the $_{\beta}Arg^{189}$, $_{\beta}Glu^{192}$ and $_{\beta}Asp^{256}$ residues complete the ion coordination through three ordered water molecules (not shown). The arginine-finger ($_{\alpha}Arg^{373}$) (orange) allows the γ-phosphate of ATP to correctly accommodate in the binding site. In *B* and *D* the aminoacid acronyms and the position of the residues interacting with ATP and the cation cofactor, are in green.

Table 1. Kinetic parameters of the F_1F_O-ATPase activity inhibition by DCCD.

	Ca-dependent	Mg-dependent
K_{DCCD} (ms^{-1})	3.8±0.4a	2.4±0.2b
$t_{½}$ (min)	10.1±0.9a	15.5±1.7b
Offset	20.5±0.9a	22.1±4.2a

The K_{DCCD} values (inhibition rate constant of DCCD) and $t_{½}$= half-life times of DCCD were calculated as detailed in Section 2.6. *Offset* is the residual F-ATPase activity in mitochondria incubated with 5 μM DCCD. Data are the mean ± SD of the values obtained from four sets of experiments carried out on distinct pools. Different letters indicate significantly different values ($P \leq 0.05$).

Table 2. F_1F_O-ATPase activities in the presence of specific inhibitors.

	Ca-dependent	Mg-dependent
Control	0.65±0.04	2.27±0.08
Vanadate	0.65±0.02	2.24±0.08
Thapsigargin	0.67±0.08	2.40±0.10
Butylhydroquinone	0.68±0.04	2.11±0.11
Oligomycin	0.04±0.01	0.06±0.01

100 μM vanadate; 1 μM thapsigargin; 10 μM butylhydroquinone; 3 μg/ml oligomycin. ATPase activities (μmoles P_i·mg protein^{-1}·min^{-1}) are the mean ± SD of three determinations on distinct mitochondrial preparations.

Figure 1

Click here to download high resolution image

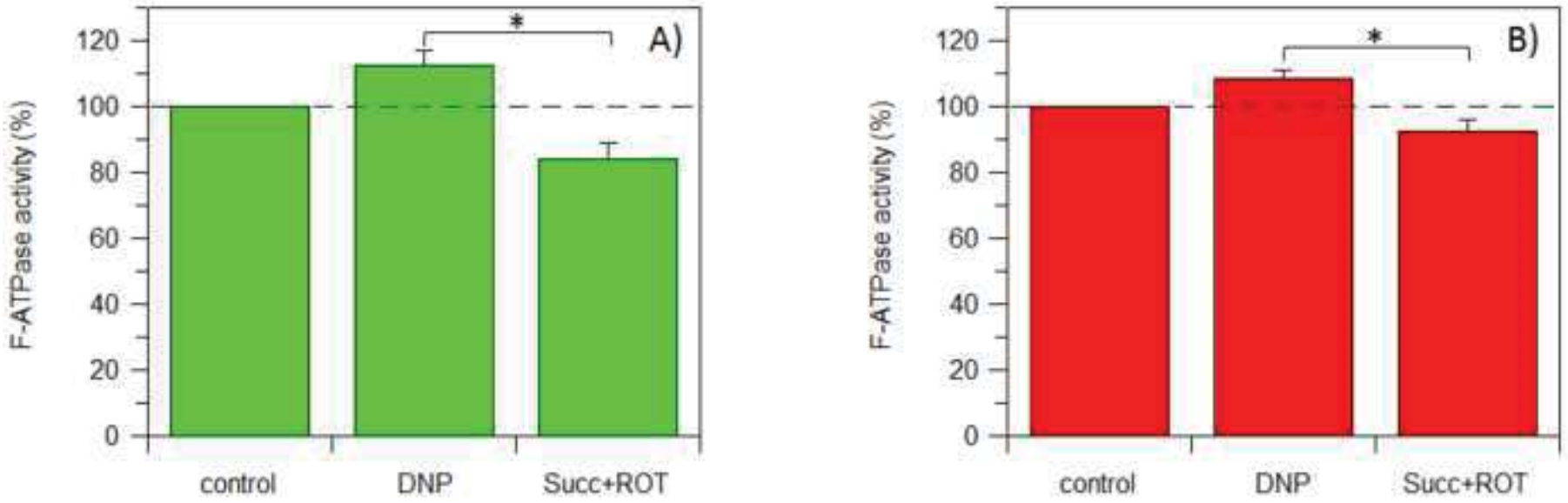

Figure 2

Click here to download high resolution image

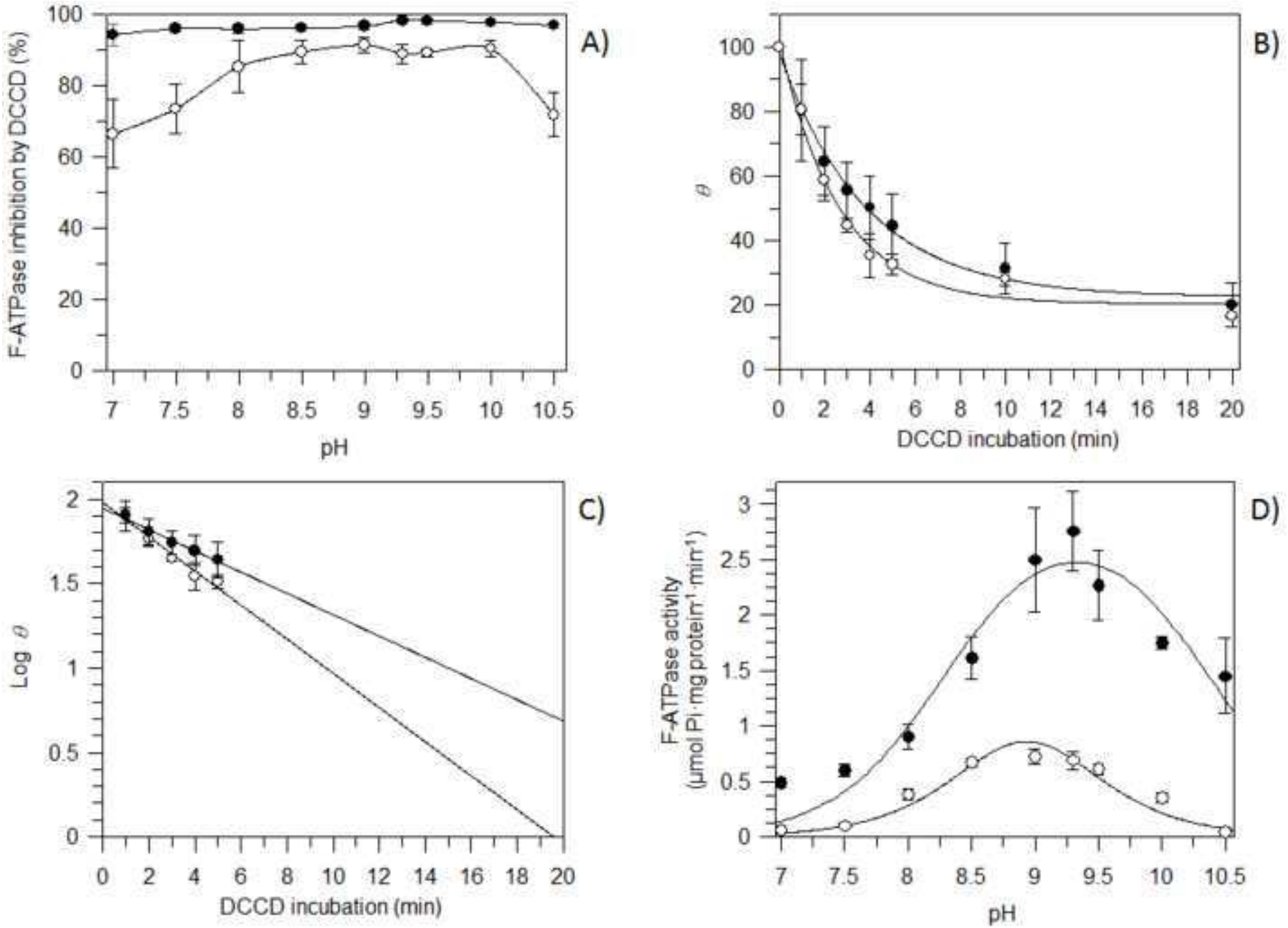

Figure 3

Click here to download high resolution image

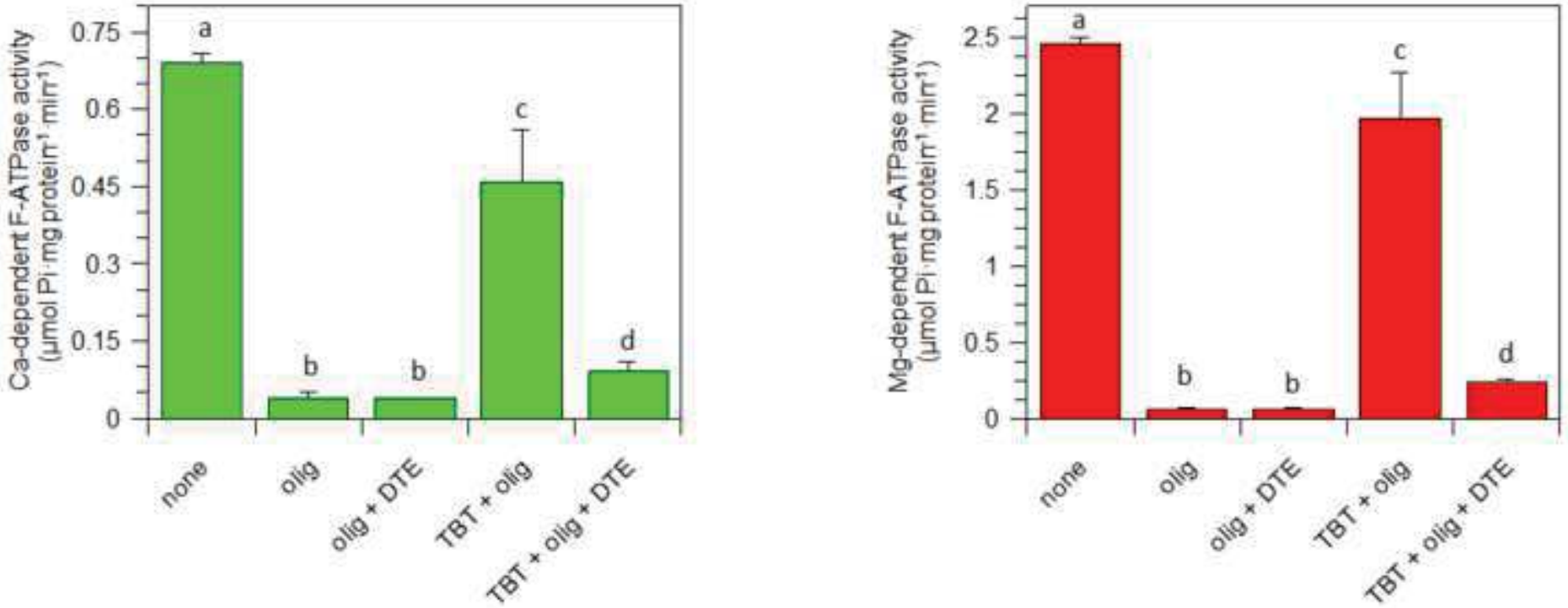

Figure 4

Click here to download high resolution image

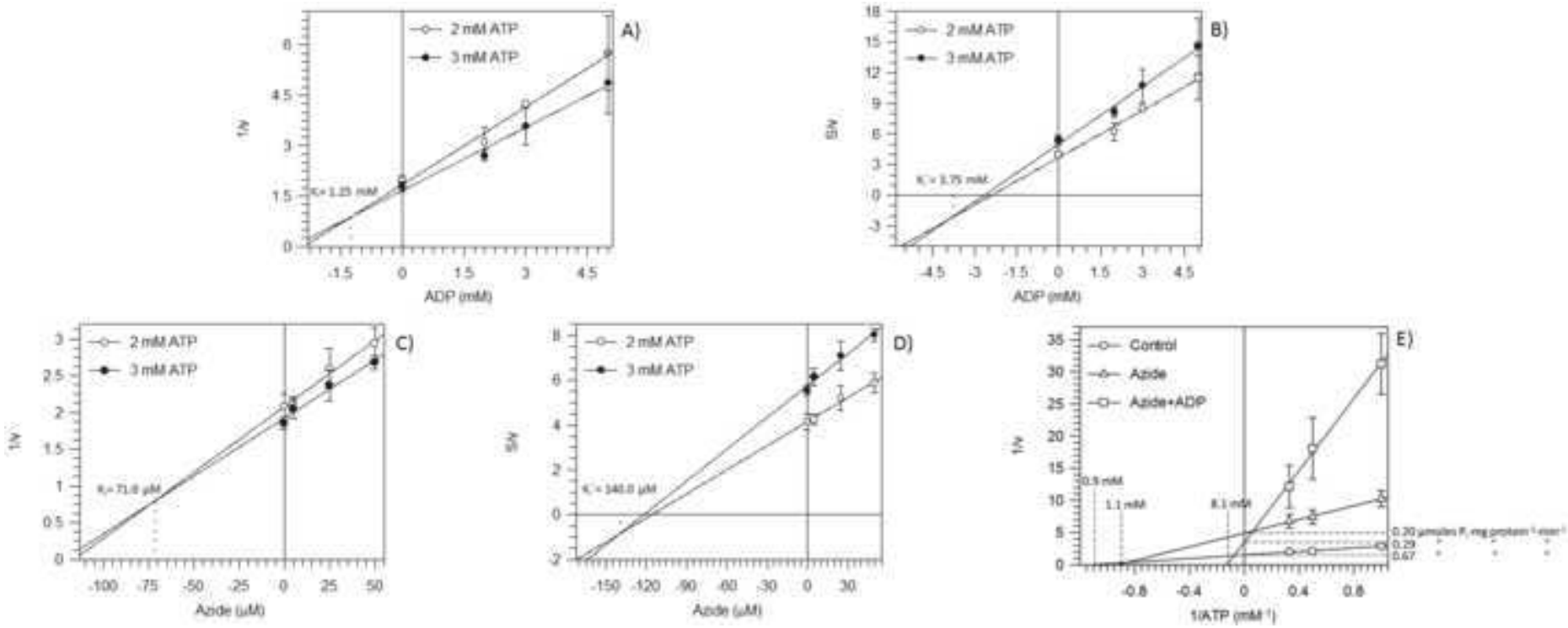

Figure 5

Click here to download high resolution image